FAR ULTRAVIOLET EMISSION CROSS SECTIONS OF Ne 11 and Ne 111 EXCITED BY ELECTRON IMPACT

Geoffrey K. James, Isik Kanik and Joseph M. Ajello

Jet Propulsion Laboratory, California institute of '1'ethnology, Pasadena CA 91109

To be submitted to: Ap.J.

ABSTRACT

We have measured the electron-impact-induced fluorescence spectrum of neon in the wavelength range 120-270nm at a spectral resolution of 0.43nm (FWHM). The strongest lines observed in the far ultraviolet (FUV) spectrum of neon arc assigned to terms of the Doublet system of Nc II ($2s^2 2p^4 nl$) and Triplet system of Ne III ($2s^2 2p^3 3l$). Our FUV spectral data obtained at 300cV electron impact energy provide absolute emission cross sections of these Ne II and Ne I II lines and arc compared to previous measurements, where available. In addition, the excitation function of the strongest Ne 11 line observed at 191 .6nm was measured from threshold to 1000cV electron impact energy.

INTRODUCTION

Electron impact-induced fluorescence spectra of neon arc of significant interest in understanding the basic physics of collisional excitation processes as well as in technological and astrophysical applications. Neon is a member of the rat-c-gas series characterized by a transition from 1, S- to jl- to jj- coupling in the spectroscopic description of the states of these atomic systems (Machado et al., 1984). Technological development of discharge systems in which neon plays an important role such as Ne-discharge light sources, He-Ne and Ne-Xe-NF_2 lasers (Sharpton et al., 1970) requires knowledge of cross sections for electron impact excitation of neon in order to model the discharge processes (Phillips et al., 1985). Neon also plays an important role in a wide range of astrophysical phenomena, being the most abundant rare-gas in the solar system, and in the cosmos after helium. Spectrophotometric observations of hot neon novae such as Nova Cygni 1992 (Shore et al. (1993), Barger et al. (1993)) and Nova V351 Puppis 1991 (Saizar et al., 1995) yield characteristic nebular emission spectra dominated by forbidden lines from multiply-ionized neon. Electron impact excitation cross sections for neon arc also needed to model the ultraviolet spectra of Ne 1, Ne II and Ne 111 from stellar atmospheres (Hubeny et al. (1991), Landini et al. (1985)), and astrophysical plasmas (Linsky (1992), Shull (1 993)).

Comprehensive reviews of previous experimental measurements of electron impact-induced emission cross sections and optical excitation functions for neon in the ultraviolet spectral region have been published most recently by van der Burgt et al. (1989) and by Heddle and Gallagher (1989). Neon, like other heavier rare-gases. has strong extreme ultraviolet (EUV) resonance lines of the type $np^5(n+1)s \rightarrow np^6$, and ion lines of the type $nsnp^6 \rightarrow ns^2np^5$. The resonance lines of Ne I at 73.59 and 74.37nm and of Ne II at 46.07 and 46.24 nm represent transitions between the lowest lying excited electronic states and the ground state of the atom and ion, respectively. in an earlier investigation (Kanik et al., 1995) we reported the EUV fluorescence spectrum of neon in the wavelength range 45-80nm produced by electron impact excitation at 300eV. Absolute emission cross sections of the EUV resonance transitions of Nc 1, Nc 11 and Nc 111 were measured, together with corresponding optical excitation functions.

In the present work our electron impact measurements are extended to cover the weaker FUV spectral region from 120- 270nm which includes transitions of the Doublet system of Ne II ($2s^2 2p^4 nl$) and Triplet system of Nc III ($2s^2 2p^3 3l$). Previous electron-impact studies of FUV transitions between excited ionic states of neon arc extremely limited, Smirnov and Sharonov (1972) measured the excitation functions of seven lines of Nc 111 corresponding to transitions between terms of tbc $2s^2 2p^3 3l$ configurations in the wavelength range 220-270nm. A subsequent publication from tbc same group (Samoilov et al., 1977) presents revised values for these cross sections. Walker and St. John (1972) measured the excitation functions of over 50 states of Nc II with an excited s, p ord electron outside a $2p^4$ core but these measurements were in the middle-ultraviolet spectral region, Smirnov and Sharonov (1973) also measured electron impact excitation functions of 38 Ne II lines in the wavelength range 270-370nm. "1'here is poor agreement between the latter two investigations. Radiative lifetimes of 37 states of Nc 1, Nc II and Nc 11 I were determined by Hesser (1968) in a modulated electron impact experiment via a phase shift analysis of their transitions in the wavelength range 200-380nm. Wc arc not aware of any previous studies of electron impact excitation of Ne II and Nc Ill lines in the FUV spectral region from 120-220nm.

Wc report in this paper the FUV fluorescence spectrum of neon in the wavelength range 120-270nm produced by electron impact excitation at 300eV. Absolute emission cross sections of the observed Nc II and Ne III lines are measured, together with the excitation function of the strongest Nc 11 line at 191.611111 from threshold to 1000cV. Possible astrophysical applications of this laboratory FUV data set for neon are discussed in Section 3.

EXPERIMENTAl, PROCEDURE

The experimental apparatus, calibration procedure, and cross section measurement technique have been described in an earlier publication (James et al., 1992). In brief, the apparatus used in the present measurements consists of an electron-impact collision chamber in tandem with a medium-resolution 1.0-m UV spectrometer. The FUV emission spectrum of neon was measured by crossing a magnetically-collimated beam of electrons at 300eV with a beam of neon gas formed by a capillary array. Emitted photons. corresponding to radiative decay of collisionally excited states of Ne II and Ne III were detected at 90° by the UV spectrometer equipped with a photomultiplier detector. The resulting FUV mission spectrum was calibrated in two stages. Firstly, the relative spectral sensitivity of the optical system and detector with wavelength was determined using the procedure described by Ajello et al. (1988) for the wavelength range 120-210nm, and by the use of a NIST-calibrated deuterium lamp source of UV spectral irradiance for the range 200-270nm. An additional normalization procedure was then applied to the spectrum in order to determine the emission cross section of each spectral feature. The absolute emission cross section of the strong Ne II line at 191.6nm, chosen to normalize the relative intensities in the FUV spectrum, was determined in a separate experiment. A gas mixture (50% Ne and 50% N_2) was admitted into the scattering chamber and the relative intensities of the Ne II line at 191.6nm and N I multiplets at 120, 149.3 and 174.3nm from dissociative excitation of N_2 were measured at 300eV electron impact energy. The absolute emission cross sections for these N I multiples at 300eV have been established by Ajello et al (1985) and James et al (1990) and provide the required normalization. For example, the emission cross section at 300eV of the strongest N I multiplet at 120nm is $(2.25 \pm 0.49) \times 10^{-18}$ cm^2.

Excitation function measurements of the Ne II line at 191.6nm, performed in a gas-swam mode by ramping the electron beam energy from threshold to 1000eV, can be put on an absolute scale by normalization to the corresponding emission cross section obtained from the spectral calibration at 300eV.

An electron impact energy of 300eV was selected for the present FUV spectral measurements to be consistent with the energy used in our earlier EUV investigation (Kanik et al., 1995). At this energy the polarization of EUV radiation from the resonance lines of Ne I is zero (Hammond et al., 1989). This is important since our spectral observations are made at an angle of 90° to the electron beam axis and would otherwise have required a correction for the polarization of the emitted EUV radiation to transform the cross section measured at 90(' to a total emission cross section.

RESULTS AND DISCUSSION

1. The FUV Emission Spectrum

Figure 1 a shows the calibrated FUV emission spectrum of neon in the wavelength range 120-270nm **produced by** electron impact excitation at 300eV, measured at a spectra! resolution of 0.43nm (FWHM). Expanded views of this spectrum are shown in Figures I b-d in which the observed lines are identified by feature numbers. The spectrum was obtained at a gas temperature of 300° K and background gas pressure of 2.5 x 10-4 Torr. Table 1 lists the 38 observed neon lines, together with the measured emission cross sections at 300eV. Wavelengths are listed to an accuracy of ± O. 1 nm. Assignments were made using the spectroscopic identifications of Kelly (1987), Bashkin and Stoner (1975), Reader and Corliss (1980) and Persson et al. (1991). Many observed features have been assigned to several unresolved spectroscopic components, listed in decreasing order of importance.

Most of the strongest lines observed in the FUV emission spectrum of neon at 300eV are assigned to terms of the Doublet system of Ne I I ($2s^22p^4 3l$ - $2s^22p^4$ n/') and Triplet system of Ne III ($2s^22p^3 3l$ - $2s^22p^3 3l'$) where / , /' = s, p, d or f. Figures 2 and 3 show simplified Grotrian diagrams of these systems of Ne II and Ne III (Bashkin and Stoner, 1975) with observed transitions indicated. Other (weaker) transitions identified in the FUV spectrum also involve the Nc II system $2s2p^6$ - $2s^22p^4[^1D]$ 3p, corresponding to features I I and 12. Feature 34 observed at 237.46nm is tentatively identified as a Nc IV transition, based on the assignment of Lindeberg (1972). It should be noted that none of the listed spectral features can be attributed to the dispersed radiation being observed in second order.

The strongest FUV emission line is feature 19 at 191 .6nm, assigned to the NeII transition $2s^22p^4[^3P]3s\ (^2P)$ - $2s^22p^4[$ 11)] 3p ($^2P^0$), with an emission cross section of 4.64 x 10-20 cm^2 at 300eV electron impact energy. This is more than two orders of magnitude lower than the corresponding cross section for the resonance line of Nc 1 at 73.59nm. In our earlier investigation of the EUV resonance lines of Nc 1 (Kanik et al., 1995) a background gas pressure of 1.0 x 10-6 Torr in the scattering chamber was chosen to ensure optically thin conditions and avoid self-absorption effects. However, the Nc 11 and Nc 111 spectral lines observed in the FUV emission spectrum arc not susceptible to these self-absorption effects. This enables a higher background gas pressure of 2.5 x 10-4 Torr to be used in order to be able to detect these much weaker emission lines. The experimental detection limit for observation of a line in the measured FUV spectrum corresponds to an emission cross section of approximately 4 x 10-22 cm^2 It should be noted that Feature I observed at 121.611111 (Lyman-α) in the FUV spectrum is produced by dissociative excitation of the trace amount of water vapor present in all vacuum systems. and is obviously not included in 'I'able 1.

The uncertainty in the absolute emission cross sections measured in this work is estimated from the square root of the sum of the squares of the following contributing errors: 1) 30% uncertainty in the relative spectral sensitivity calibration, 2) 22% uncertainty in the N I 120nm emission cross section (James et al., 1990) and 3) up to 10% uncertainty due to signal statistics. This calculation yields on overall error of approximately 39%

Previous electron-impact studies of FUV transitions between excited ionic states of neon arc extremely limited. Smirnov and Sharonov (1972) measured the excitation functions of seven lines of Nc I I I from threshold to 500eV corresponding to transitions between terms of the

$2s^2 2p^3 3l$ configurations. These lines arc observed in the wavelength range 220-270nm and correspond to features 29, 30 and 35-39 in our FUV spectrum. A subsequent publication from the same group (Samoilov et al., 1977) presented revised measurements of some of these cross sections and determined the cascade contribution to the population of one of the levels (feature 39). Their stated absolute accuracy was 40%. It should be pointed out that all the emission cross sections measured in the present work include any cascade contribution to tbc population of the upper excited level.

"1'able 2 shows a comparison of the FUV emission cross sections measured in the present work at 300cV to the data of Smirnov and Sharonov (1972) and Samoilov et al. (1977). There is not good agreement between the three data sets, the cross sections measured by Smirnov and co-workers being of the order of 75°/0 higher than tbc present values. With the exception of features 30 and 39, however, the large stated error bars do overlap. Note that in a separate middle ultraviolet (MUV) investigation of Nc II tbc cross section values measured by Smirnov and Sharonov (1973) were, on average, three times larger than those measured by Walker and St. John (1972) for the same transitions and the spread was very large. Wc arc not aware of any previous studies of electron impact excitation of Ne II and Ne III lines in tbe FUV spectral region from 120-220nm.

2, Excitation Function of the Ne II line at 191.6nm

Figure 4 shows the absolute excitation function of the strongest Nc II line at 191.611111 (Feature I 9) measured at a spectral resolution of 0.43nm (FWHM) from threshold to 1000cV electron impact energy. This line is assigned to the NeII transition $2s^2 2p^4 [^3P]$ 3s (^2P) - $2s^2 2p^4 [^1D]$ 3p (2P()) . Excitation of tbe upper level of this transition nominally involves the simultaneous ionization of onc 2p electron and excitation of another, resulting in a threshold excitat ion energy (appearance potential) of 55.82eV. Relative excitat ion function data were placed on an absolute scale by normalization at 300eV electron impact energy to the emission cross section value of **4.64 x** 10^{-20} cm^2 obtained in our FUV spectral calibration. Also shown in Figure **4** is a modified Born approximation analytic fitting function applied to the data in the manner described in detail by Shemansky et al. (1985 a, b). Fitting constants are given in the Figure caption. We are not aware of any previous excitation function measurements of this transition. For comparison, however, measurements by Rapp and Englander-Golden (1 965) of the total ionization cross section of neon are shown in Figure 5 and exhibit a similar energy dependence of the relative cross section.

Simultaneous ionization and excitation is optically forbidden whenever it involves a two-electron process. Based on the stated assignment of the upper level of the Ne II transition at 19 1.6nm, the corresponding excitation function is thus expected to exhibit dipole-forbidden behavior in the high energy region. However, the measured shape is characteristic of a dipole-allowed process (verified by the finite value for the Born coefficient C_7 in the analytic fit applied to the data). In contrast, comparable excitation functions measured for He II and Ar II transitions also involving simultaneous ionization and excitation demonstrate the expected optically forbidden behavior in the high energy region (Shemansky et al. (1985b), Ajello et al. (1990)), The **neon total** ionization cross section data of Rapp and Englander-Golden (1965) is dominated by the optically allowed single electron process $2s^2 2p^6$ - $2s^2 2p^5$ and its high energy dependence is also as expected. A possible explanation for the anomalous shape of the Ne II 19 1.6nm excitation function involves configuration interaction in which the nominal upper level of this transition may be strongly coupled to an (unidentified) degenerate state populated by an optically allowed process involving a single inner-shell electron.

Emission cross sections reported in this work will include any cascade contribution to the population of the upper level. For the case of the transition at 19 1.6nm, possible cascade channels are from higher lying $2s^2 2p^4 nl$ levels , though no measurements are available to quantify these possible contributions. Excitation of these cascade channels will also involve two- electron processes.

Measurements of emission cross sections (Q_{90^o}) made at an angle of 90^O between the electron beam and optic axis arc related to the total emission cross section ((.)$_{(otal}$) by $Q_{total} = Q_{90^o} / (1-P/3)$, where P is the polarization of the emitted radiation. I lammond et al. (1989) measured the polarization of the integrated radiation emitted following electron impact excitation of Nc in the energy range from threshold to 480eV. This polarization data was used to correct our previous measurements of EUV excitation functions of the strongly polarized Nc I resonance lines (Kanik et al. 1995). Similar polarizat ion correction was not applied to the present FUV excitation function of the Nc 11 line at 191.611111 since the polarization data of I lammond et al. (1989) arc restricted to the integrated EUV radiation channels by their choice of photon detector. Furthermore, Walker and St. John (1972) examined polarization effects in an investigation of MUV excitation functions of over 50 slates of Nc II with an excited s, p or d electron outside a $2p^4$ core. They found only 3 transitions with polarizations of more than 5°/0, and all were less than 10O/O.

3. **Astrophysical Applications**

I'here arc a number of possible astrophysical applications for the laboratory FUV data set of neon measured in the present work. Neon abundance is important for tracing the effects of core nucleosynthesis in intermediate mass stars, especially the progenitors of novae, and in the interpretation of the spectra of supernovae in their early stages of outburst (Baron et al. (1 994), Nugent et al. (1995), Eastman and Pinto (1993), Eastman et al. (1994)). In a study of tbc UV spectral evolution of Nova Cygni 1992, Shore et al, (1993) rc-assigned tbc line observed at 2 15nm to a permitted Nc III transition. This neon line is also observed in our laboratory spectrum (Feature 26), supporting their revised analysis, In another application, the 191 .6nm line appears to explain the high resolution emission line profile near (' III in Nova Her 1991 (Shore, private communication, 1995). Lines observed near 191nm arc important because of their possible contribution to low resolution spectra of planctary nebulae where the C III / Si III ratio is used to determine electron densities (Nussbaumer and Stencel, 1989). Finally, in another recent nova (Aql 1995), observation of a UV line at 194nm (Shore, private communication, 1995) might be attributed to the Ne II transition measured in our spectrum (Feature 21). Laboratory FUV data for neon may also assist in the accurate identification of lines observed in the FUV spectra of novae where NeII and NeIII wavelengths may coincide with the spectral signatures of other species that arc normally expected to be overabundant in the ejecta. Non-LTE model calculations of the early optically thick dense stages of nova and wind spectra also require knowledge of the permitted transitions of neon in its lower states of ionization (Hauschildt et al. (1994, 1995), Wu et al. (1992), Shore (1992)).

Collision cross sections for excitation of high-lying states of Ne II and Ne III are especially important for the interpretation of massive white dwarf spectra, where the densities are high and collisional excitation produces appreciable populations in these excited states. Recent 11011 -1,'1' E calculations arc discussed by Hubeny et al. (1991) for high gravity stars. Determinations of opacities in plasmas of any white dwarf via the mission spectra of the surrounding gas rely cm the availability of accurate experimental collision cross section data (Ferland , 1994).

laboratory measurements of the electron-impac.t-induced FUV emission spectrum of neon may also be important in the analysis of dielectronic recombination in solar and stellar coronae (Linsky, 1992) and for the analysis of the UV spectra of dense hot Magellanic Cloud planetary nebulae (Dopita and Meatheringham (1991 a, b), Dopita et al. (1993)).

ACKNOWLEDGMENTS

This work was carried out at the Jet Propulsion laboratory, California institute of Technology and was supported by NASA Planetary Atmospheres, Astronomy/Astro physics and Space Physics Program Offices, the Air Force office of Scientific Research (AFOSR) and the Aeronomy Program of tbc National Science Foundation. The authors benefited greatly from discussions with Steve Shore of Indiana University South Bend.

REFERENCES

J.M. Ajello, G.K. James, B. Franklin and S. Howell, J. Phys. B: At. Mol. Opt. Phys. 23, 4355 (1990).

J. M. Ajello and D. E. Shemansky, J. Geophys. Res. 90,9845 (1985).

J.M. Ajello, D.E. Shemansky, B.O. Franklin, J. Watkins, S. Srivastava, G.K. James, W.T. Simms, C. W. Hord, W. Pryor, W. McClintock, V. Argabright and D Hall, Appl. Opt. 27,980 (1988).

A. J. Barger, J. S. Gallagher, K. S. Bjorkman, K. A. Johansen and K. H. Nordsieck, Ap.J 419, 1,85 (1993).

E. Baron, P.H. Hauschildt and D. Branch, Ap.J 426, 334 (1994).

S. Bashkin and J. O. Stoner, "Atomic Energy Levels and Grotrian Diagrams", pub. North Holland Publishing Co., vol 1,300 (1975).

P. J. M. van der Burgt, W. B. Westerveld and J. S. Risley, J. Chem. Ref. Data 18, 1757 (1989).

M.A. Dopita, H.C. Ford, R. Bohlin, I.N. Evans and S.J. Meatheringham, Ap.J 418, 804 (1991 b).

M.A Dopita and S.J. Meatheringham, Ap.J 367, 115 (1 991a).

M.A. Dopita and S.J. Meatheringham, Ap.J 377. 480 (1 991 b).

R.G. Eastman and P.A. Pinto, Ap.J 412, 73 I (1993).

R. G. Eastman, S.E. Woolsey, T.A. Weaver and P.A. Pinto, Ap.J 430, 300 (1994).

G. Ferland, CLOUDY: A Nebular Photoionization Code, Ohio State University (1994).

P. Hammond, W. Karras, A. G. McConkey and J. W. McConkey, Phys. Rev. A 40, 1804 (989).

P. 1. Hauschildt, S. Starrfield, S. Austin, R.M. Wagner, S.N. Shore and G. Sonneborn, Ap. J. 422,831 (1994).

P. H. Hauschildt, S. Starrfield, S.N. Shore, F. Allard and E. Baron, Ap. J, In Press (1995).

D. W. O. Heddle and J. W. Gallagher, Rev. Mod. Phys. **61**, 22 I (1989).

J.E. Hesser, Phys. Rev 174,68(1 968).

1. Hubeny, S.R. Heap and B. Altner, Ap.J 377, L33 (1991).

G. K. James, J. M. Ajello, B. Franklin and D. E. Shemansky, J. Phys. B: At. Mol. Opt. Phys. 25, 2055 (1 990).

G. K. James, J. M. Ajello, 1. Kanik, B. Franklin and D.E. Shemansky, J. Phys. B: At. Mol. Opt. Phys. **25** , 1481 (1992).

1. Kanik, J. Ajello and G. K. James, submitted to Phys. Rev. A (1995).

R. L. Kelly, J. Chem. Ref. Data 16,35 (1987).

M. Landini, B. C. Fossi, F. Paresce and R. Stern, Ap. J. 289, 709(1985).

S. Lindeberg, Uppsala University Institute of Physics Report No. UUIP-758 (1972) (unpublished).

J. 1. Linsky, in "Atomic and Molecular Data for Space Astronomy: Needs, Analysis, and Availability", ed. P. L. Smith and W. Wiese, Lecture Notes in Physics 407, Berlin: Springer-Verlag, 33 (1992).

L. E. Machado, E. P. Leal and G. Csanak, Phys. Rev. A 29, 1811 (1984).

P. Nugent, E. Baron, P. H. Hauschildt and D. Branch, Ap.J 441, L33 (1 995).

11. Nussbaumer and R. Stencel, in " Exploring the Universe with the IUE Satellite", ed. Y. Kondo, Dordrecht: Kluwer, (1989).

W. Persson, C.G. Wahlstrom , 1,. Jonsson and H.O. Di Rocco, Phys. Rev. A 43,4791 (1991).

M. Il. Phillips, L. W. Anderson and C. C. Lin, Phys. Rev. A 32,2117 (1985).

D. Rapp and P. Englander-Golden, J. Chem. Phys. 43, 1464 (1965).

J. Reader and C. 11. Corliss, "Wavelengths and Transition Probabilities for Atoms and Atomic Ions", Nat, Stand. Ref. Data Ser., Nat. Bur. Stand. **68**, U.S. GPO, Washington, DC (1980).

f'. Saizar, R.E. Williams, 1. Pachoulakis, E. Rostschild, S.N. Shore, S. Starrfield, R. Gonzalez-Riestra and G. Sonneborn, MNRAS preprint: " Nova V351 Puppis 1991: A Multiwavelength Study of the Nebular Phase", (1995).

V. P. Samoilov, Yu. M. Smirnov and G. S. Starikova, opt, Spectrosc (USSR) 42,22 (1977).

F. A. Sharpton, R. M. St.John, C. C. Lin and F. E. Fajen, Phys. Rev. A 2, 1305 (1970).

D. E. Shemansky, J. M. Ajello and D. 1'. Hall, Ap. J. 296.765 (1985a).

D. E. Shemansky, J. M. Ajello, D. "1'. Hall and B. Franklin, Ap. J. 296, 774 (1985 b).

S. N. Shore, in "Atomic and Molecular Data for Space Astronomy: Needs, Analysis, and Availability", ed. P. L. Smith and W. Wiese , Lecture Notes in Physics 407, Berlin:Springer-Verlag, 7 (1992).

S.N. Shore, G. Sonneborn, S. Starrfield, R. Gonzalez-Riestra and T.B. Ake, Ap.J 106,2408 (1993).

J. M Shull, Physics Scripts 147, 165 (1993).

Yu.M. Smirnov and Yu. I). Sharonov, Opt. Spectrosc.(USSR) 32,333 (1972).

Yu. M. Smirnov and Yu. D. Sharonov, Sov. Astron. 16, 900 (1973).

K.G Walker and R.M. St.John, Phys.Rev.A 6,240 (1972).

C.C. Wu, G.A. Reichert, '1'.11. Ake, A. Boggess, A.V. Holm, C. L. Imhoff, Y. Kondo, J.M. Mead and S.N. Shore, "international (Ultraviolet Explorer (IUE) Ultraviolet Spectral Atlas of Selected Astronomical Objects", NASA Ref. Pub. 1285, iv +421 pp. (1992).

FIGURE CAPTIONS

Figure 1: (a) Calibrated FUV emission spectrum of neon produced by electron impact excitation at 300 eV, measured at a spectral resolution of 0.43nm (FWHM) in the wavelength range 120-270nm. Expanded views of this 300eV spectrum are shown in (b) 120-17511111, (c) 170 -22 S11111 and (d) 215-270nm. The spectrum was measured in a cmscd-beam mode at a background gas pressure of 2.5×10^{-4} Torr. Identifications and absolute emission cross sections of the observed features (numbered) are listed in "1'able 1. The accuracy of the wavelength scale is ±0.1nm.

Figure 2: Simplified Grotrian diagram for the prominent FUV transitions of neon showing transitions between terms of the Doublet system of Ne 1 I [$2s^2 2p^4 3l$ - $2s^2 2p^4 nl'$] observed in the wavelength range 120-270nm (Bashkin and Stoner, 1975)

Figure 3: Simplified Grotrian diagram for tbe prominent FUV transitions of neon showing transitions between terms of the Triplet system of Ne 111 ($2s^2 2p^3 3l$ - $2s^2 2p^3 3l'$) observed in the wavelength range 120-270nm (Bashkin and Stoner, 1975)

Figure 4: Absolute excitation function of the Ne 11 line at 191.6nm measured at a spectral resolution of 0.43nm (FWHM) from threshold to 1000eV electron impact energy (dots); the appearance potential is at 55.82eV. Solid line represents a modified Born approximation analytic fitting function (Shemansky et al. 1985a, b) applied to the data [with fitting constants ($\times 10^{-16}$): C_0 = O, C_1= 0.019839, $C_2 = C_3 = C_4$ = O , C_5 = -0.1277, C_6= 0.1277, C_7= 0.12915 and alpha= 0.22388].

Figure 5: Absolute Total ionization cross section of neon measured by Rapp and Englander-Golden (1965) from threshold (21.56eV) to 1000eV electron impact energy.

Calibrated FUV Emission Spectrum of Ne produced by 300eV Electron Impact

[AA = 0.43 nm]

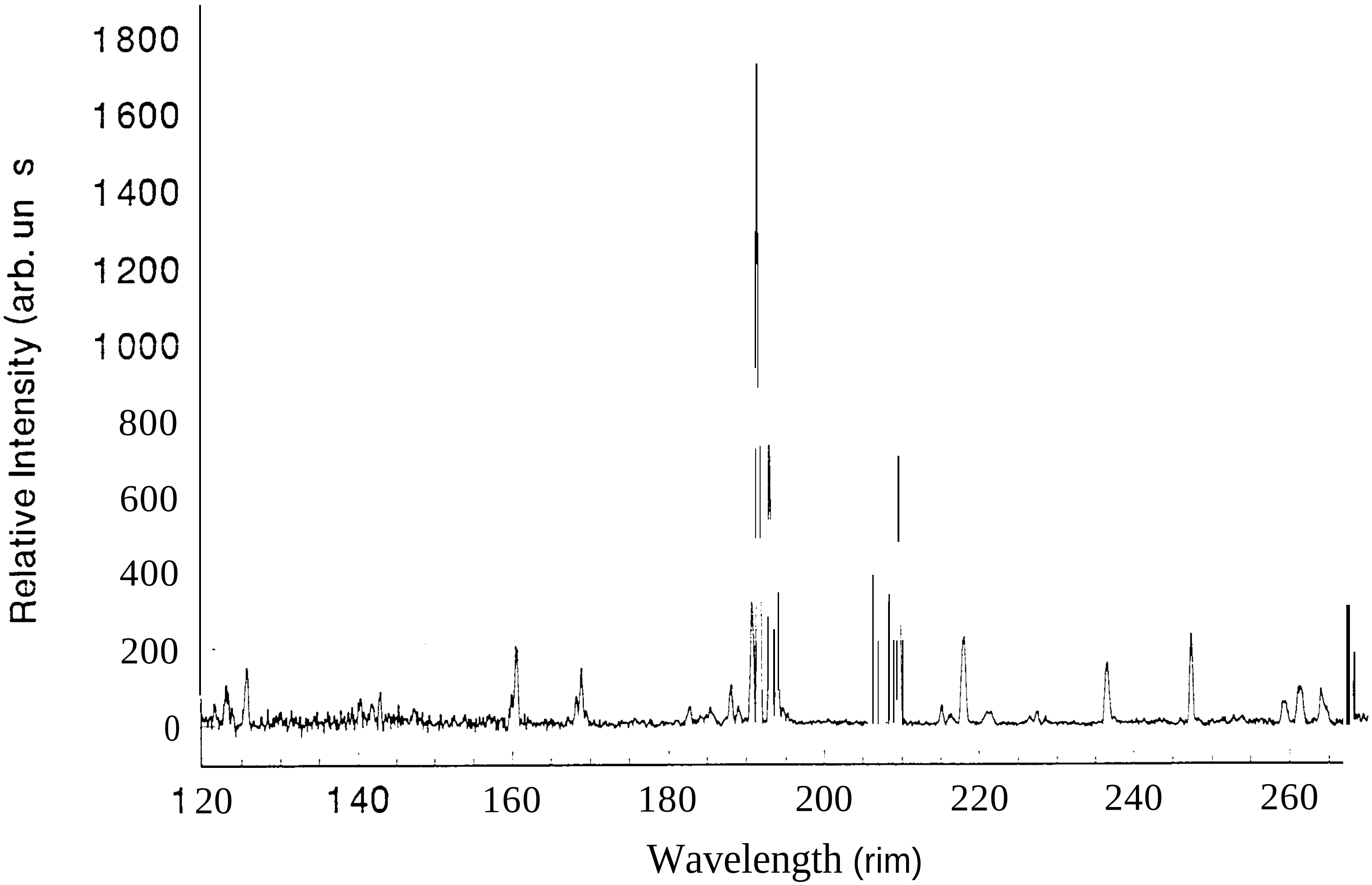

Figure 1a.

Calibrated FUV Emission Spectrum of Ne produced by 300eV Electron Impact

[$\Delta\lambda = 0.43$ nm]

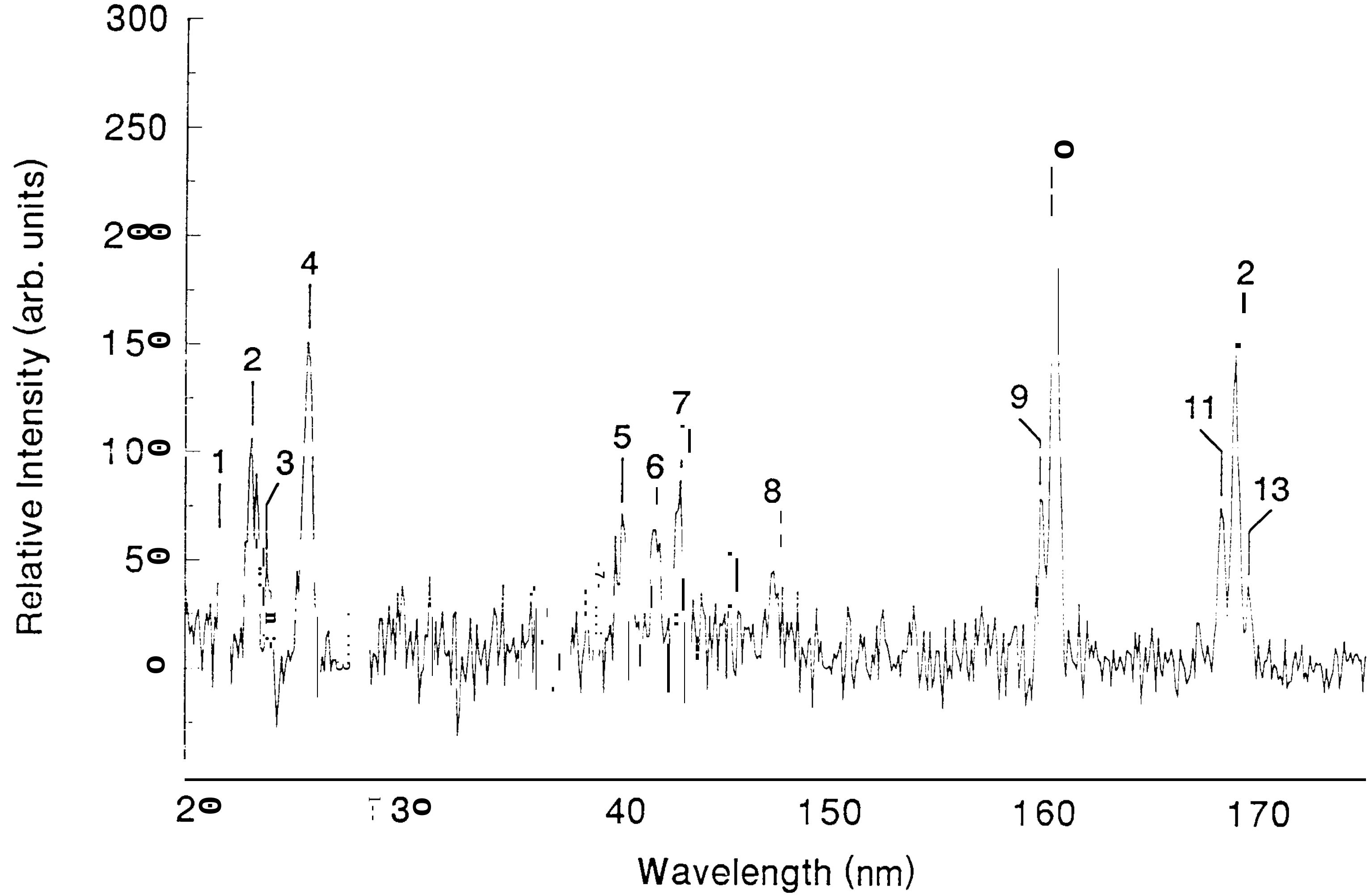

Figure 1b

Calibrated FUV Emission Spectrum of Ne produced by 300eV Electron Impact

[$\Delta\lambda$ = 0.43 nm]

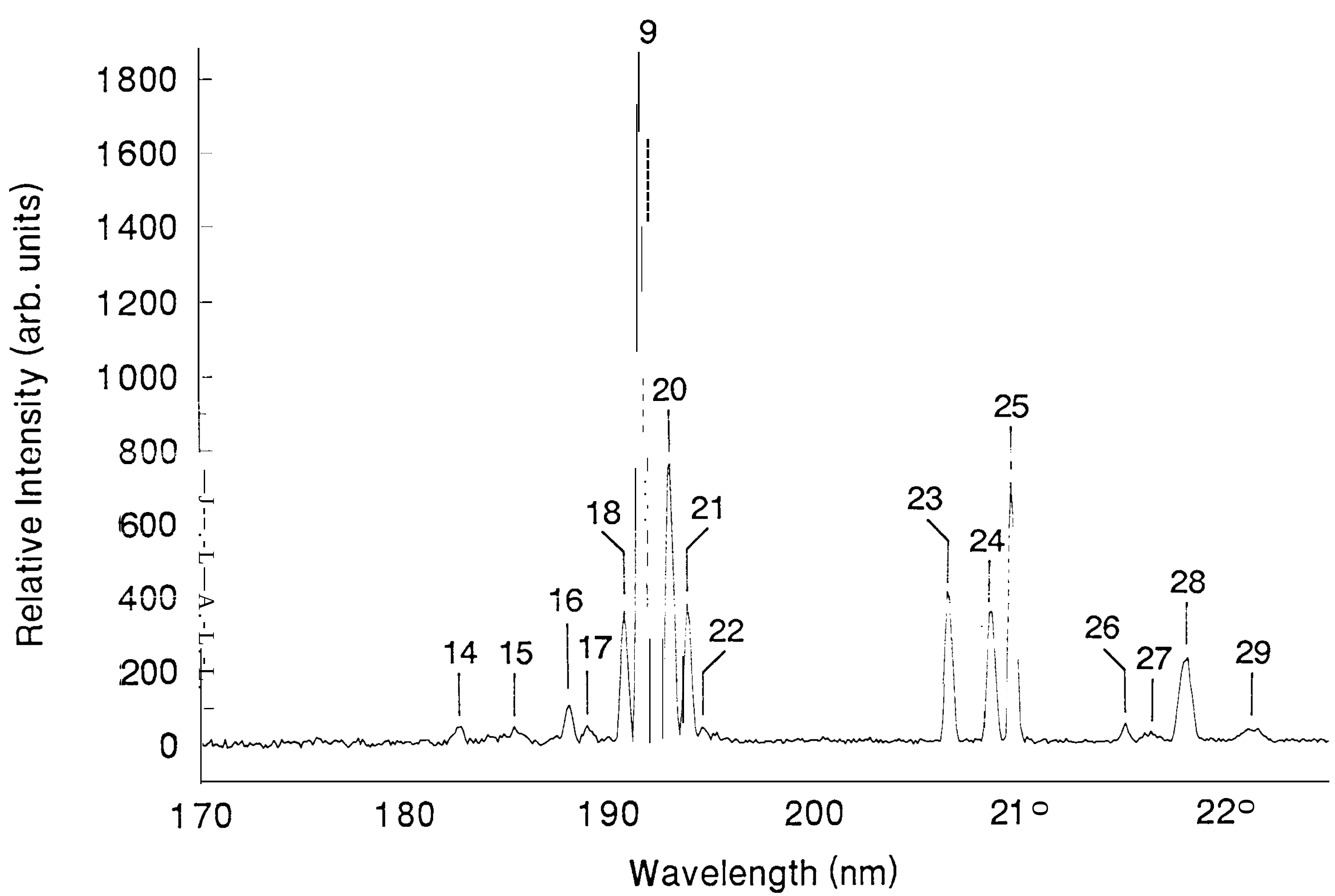

Figure 1c

Calibrated FUV Emission Spectrum of Ne produced by 300eV Electron Impact

[$\Delta\lambda = 0.43$ nm]

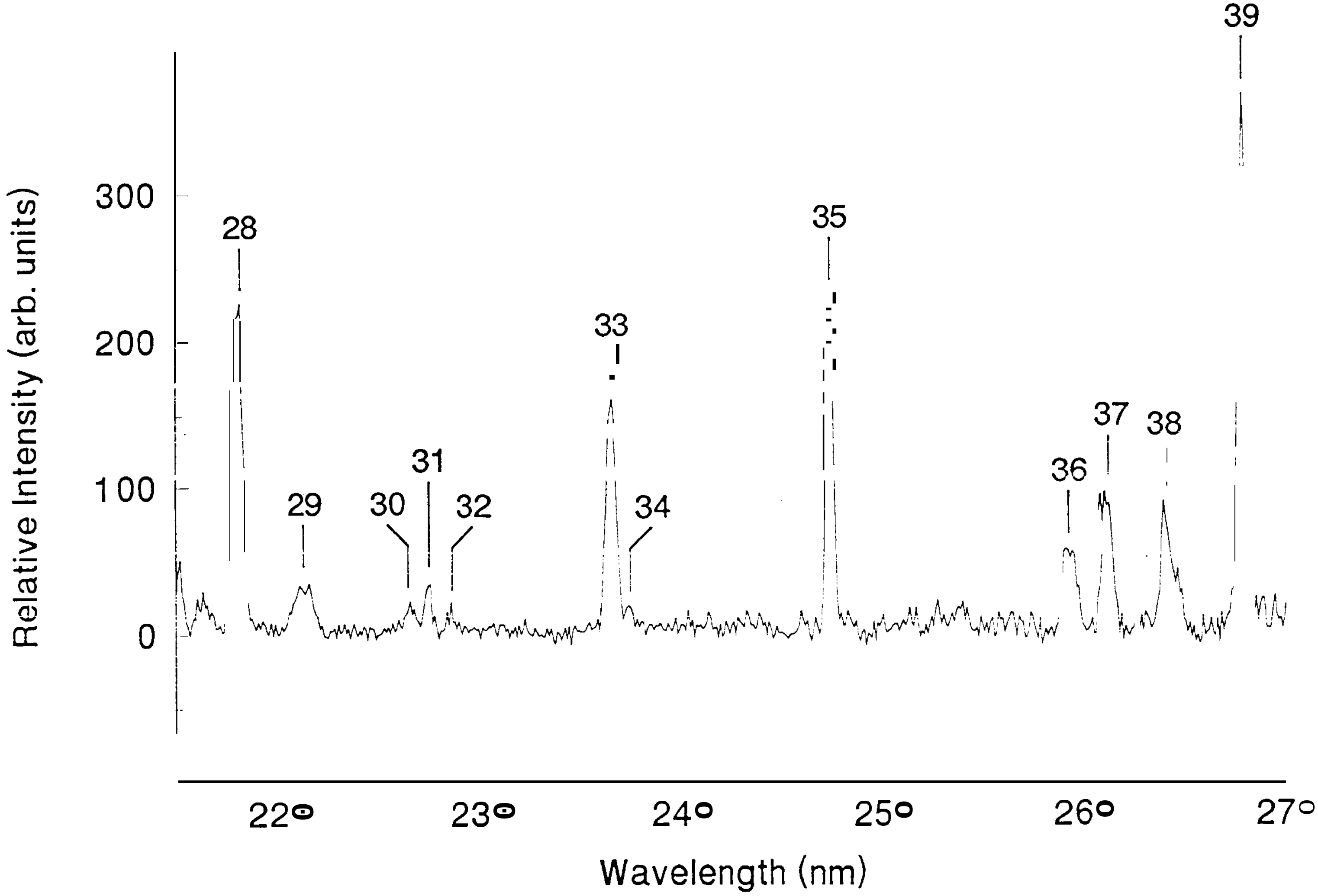

Figure 1d

Figure 2

Ne II GROTRIAN DIAGRAM

(Configuration: $ls^2 2s^2 2p^4$ nl. Doublet System)

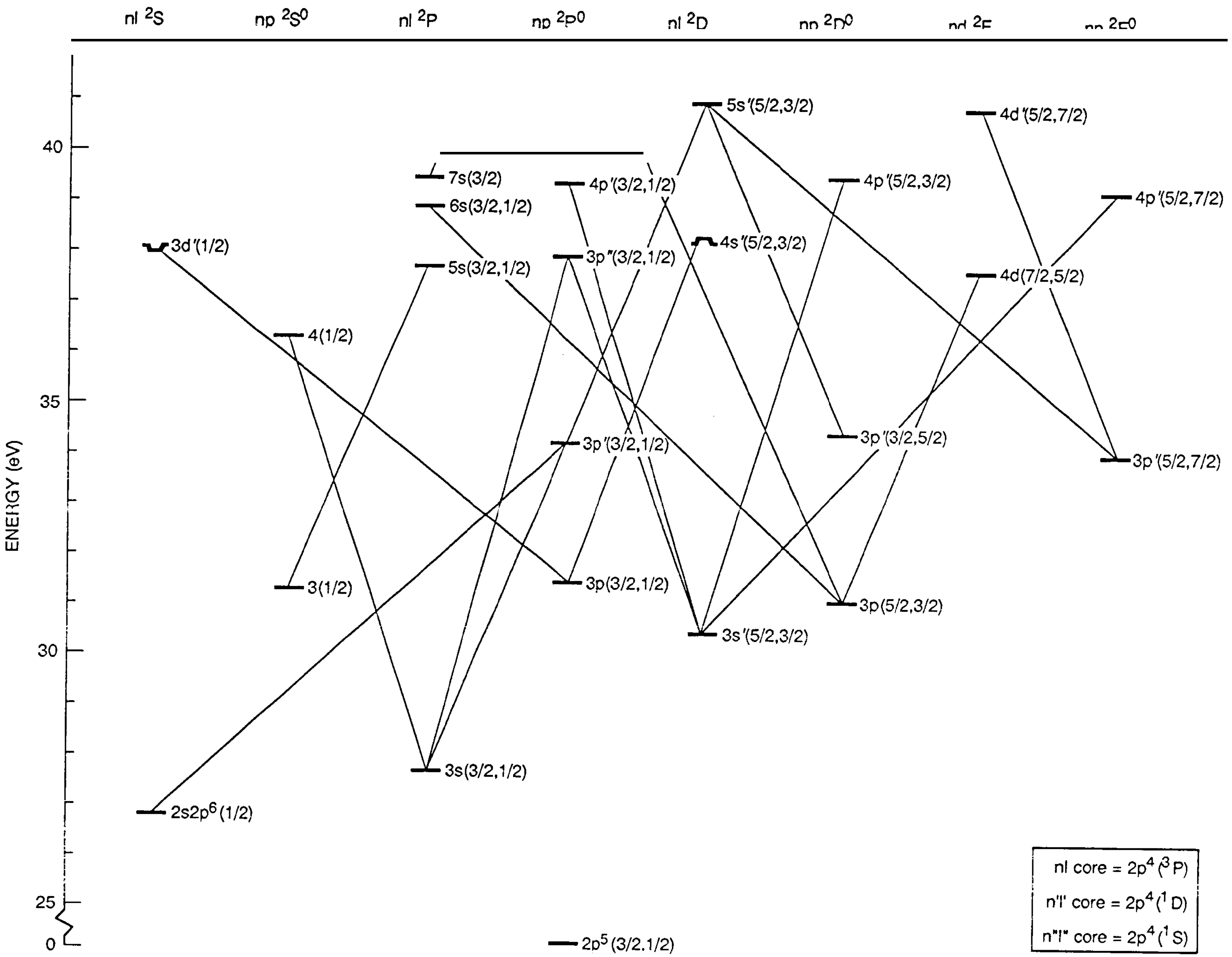

Figure 3

Ne III GROTRIAN DIAGRAM
(Configuration: $1s^22s2\ 2p^3$ 31, Triplet System)

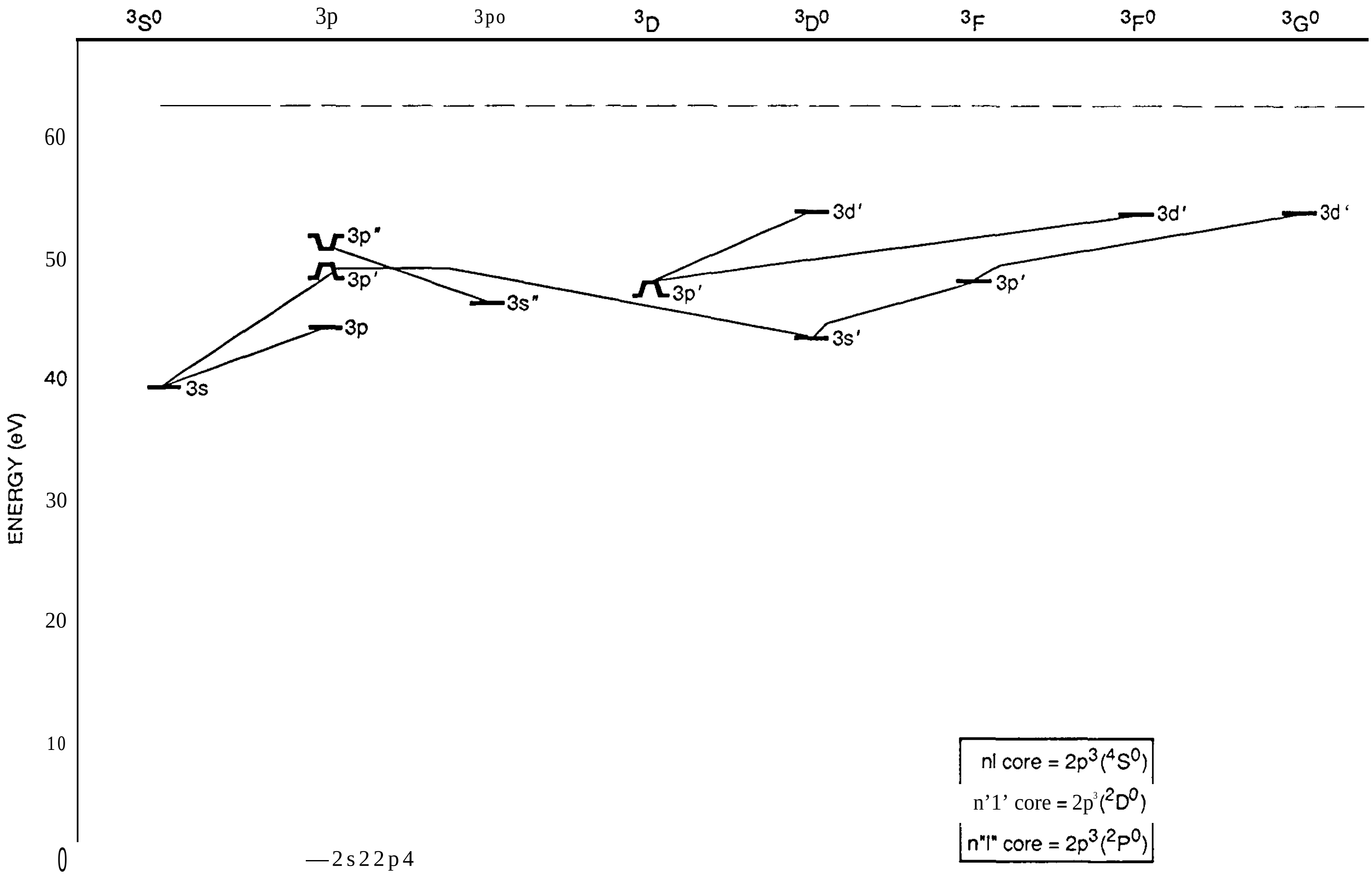

Figure 4

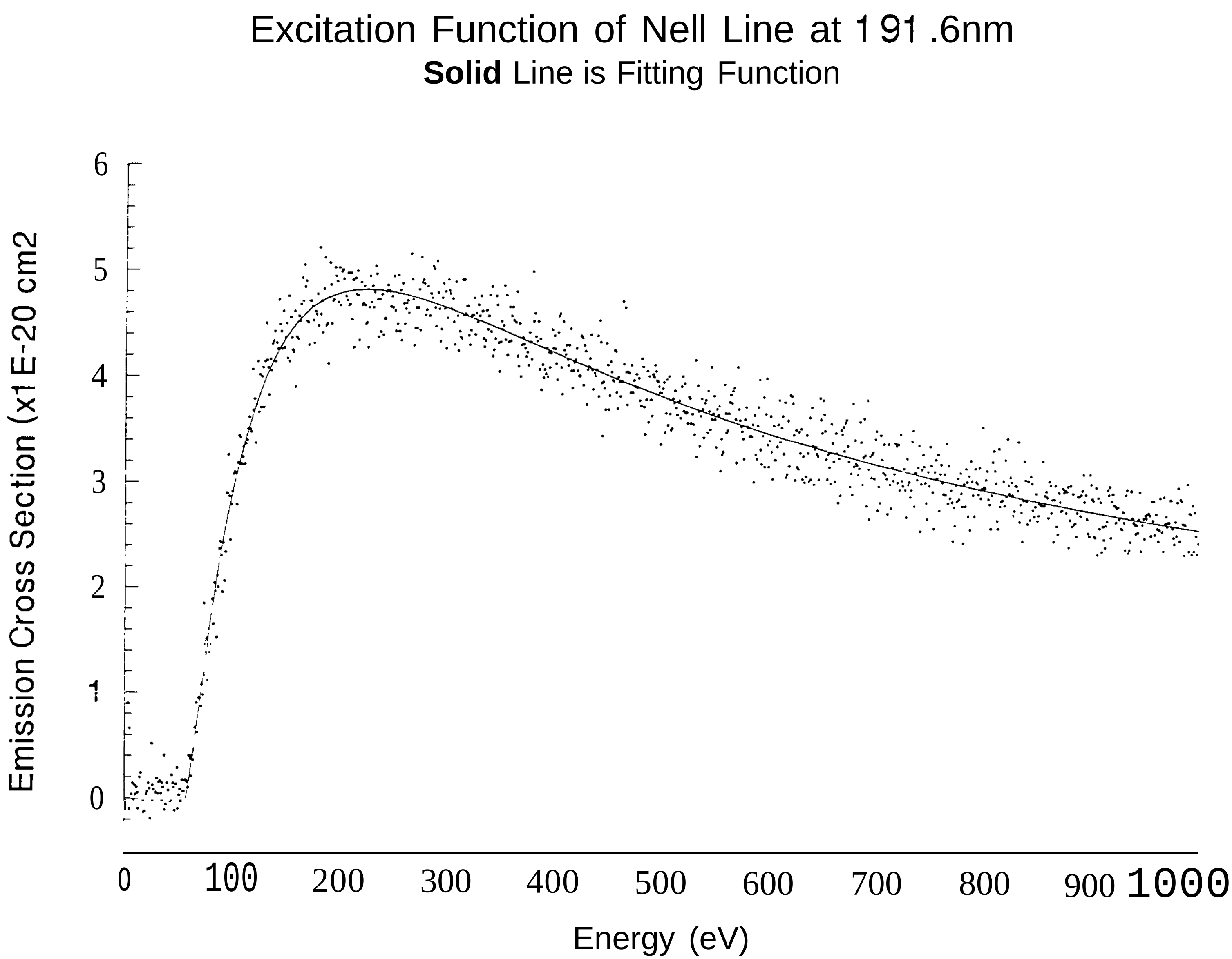
Excitation Function of NeII Line at 191.6nm
Solid Line is Fitting Function
Emission Cross Section (x1E-20 cm2
0
1
2
3
4
5
6
0
100
200
300
400
500
600
700
800
900
1000
Energy (eV)

Figure 5

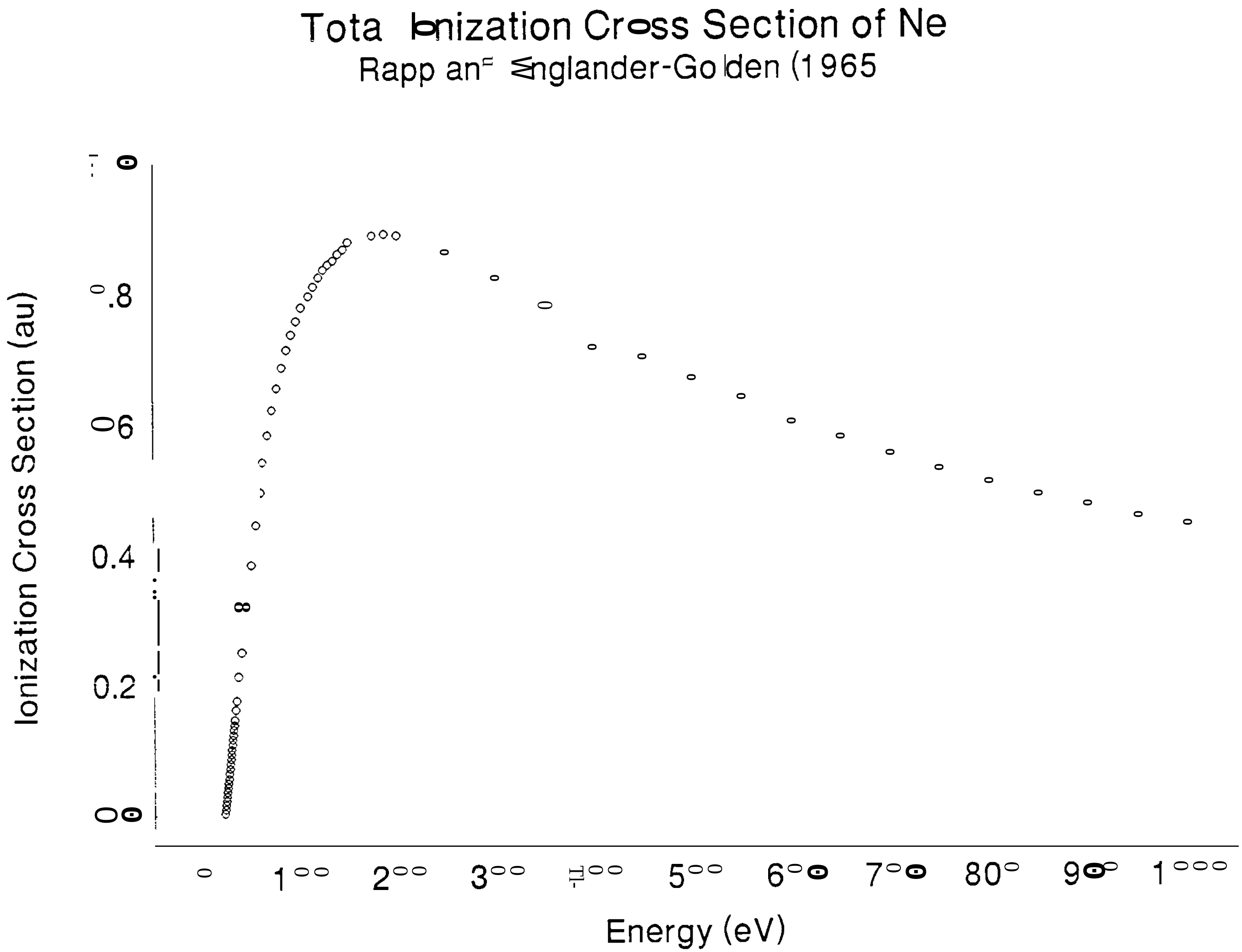

Total Ionization Cross Section of Ne
Rapp and Englander-Golden (1965
Ionization Cross Section (au)
0.2
0.4
0.6
0.8
Energy (eV)
100
200
300
500
1000

TABLE I ABSOLUTE EMISSION CROSS SECTIONS OF NEON AT 300 eV ELECTRON IMPACT ENERGY

Feature Number	Species	integrated λ (ml)	Observed Peak λ (rim)	Configuration	Term	Emission Cross Section (x 10^{-2}' cm^2)
2	Ne II	122.66-123.46	123.06	$2s^22p^4(^3P)3s - 2s^22p^4(^1S)3p$	$2_p - {}^2P^0$	3.39
	Ne III			$2s^22p^3(^2D)3s - 2s^22p^3(^4S)4p$	$^3D - {}^3P$	
3	Nc 11	123.56-124.06	123.76	$2s^22p^4(^3P)3s - 2s^22p^4(^1S)3p$	$^2P - {}^2P^0$	0.89
	Ne III			$2s^22p^3(^2D)3p - 2s^22p^3(^2P)4s$	3p - 3p	
4	Ne 111	125.06-125.96	125.66	$2s^22p^3(^4S^0)3s - 2s^22p^3(^2D^0)3p$	$^3S^0 - {}^3P$	5.07
5	Nc II	139.86-140.56	140.26	$2s^22p^4(^1D)3s - 2s^22p^4(^1D)4p$	$^2D - {}^2P^0, {}^2D^0$	2.17
				$2s^22p^4(^3P)3s - 2s^22p^4(^3P)4p$	4p - 4po	
6	Nc 11	141.46-142.26	141.76	$2s^22p^4(^1D)3s - 2s^22p^4(^1D)4p$	$^2D - {}^2F^0$	1.99
				$2s^22p^4(^3P)3s - 2s^22p^4(^3P)4p$	$4_p - {}^4P^0$	
7	Nc II	142.56-143.16	142.96	$2s^22p^4(^3P)3s - 2s^22p^4(^3P)4p$	‘P - $^2P^0$	1.97
	Ne III			$2s^22p^3(^2P)3p - 2s^22p^3(^2P)4s$	$^3S - {}^3P$	
8	Ne II	146.76-147.56	147.36	$2s^22p^4(^3P)3s - 2s^22p^4(^3P)4p$	2p - $^2S^0$	1.56
				$2s^22p^4(^3P)3p - 2s^22p^4(^3P)7s$	$^21)^0 - {}^2P$	
	Nc 111			$2s^22p^3(^2D)3p - 2s^22p^3(^2D)4s$	$^1F - {}^1D$	
				$2s^22p^3(^4S)3d - 2s^22p^3(^4S)5p$	$^5D - {}^5P$	
9	Ne II	159.46 - 59.96	159.81	$2s^22p^4(^1D)3s - 2s^22p^4(^3P)5p$	$^2D - {}^2P^0$	1.72
				$2s^22p^4(^3P)3p - 2s^22p^4(^3P)6s$	$^2D^0$ - 2p	
	Ne III			$2s^22p^3(^4S)4p - 2s^22p^3(^4S)8s$	$^5P - {}^5S$	
10	Nc 11	160.06-160.85	160.46	$2s^22p^4(^1D)3s - 2s^22p^4(^3P)5p$	$^2D - {}^2P^0$	6.21
	Nc III			$2s^22p^3(^2D)3s - 2s^22p^3(^2P)3p$	‘I)- ‘I)	
11	NeII	167.76-168.36	168.16	$2s2p^6 - 2s^22p^4(^1D)3p$	^2S - 2po	1.78
				$2s^22p^4(^3P)3p - 2s^22p^4(^3P)6s$	2po - 2p	
12	Ne II	168.46-169.16	168.86	$2s2p^6 - 2s^22p^4(^1D)3p$	^2S - 2po	3.93
	Ne III			$2s^22p^3(^2D)3s - 2s^22p^3(^2P)3p$	$^3D - {}^3D$	
				$2s^22p^3(^2D)3p - 2s^22p^3(^4S)4d$	‘1)- ^3D	

Feature Number	Species	Integrated λ ([1111])	Observed Peak λ (rim)	Configuration	Term	Emission Cross Section (x 10⁻²' cm²)
13	Nc 11	169.26-169.76	169.46	$2s^22p^4(^1D)3s$ - $2s^22p^4(^1S)3p$	^2D - $^2P^0$	0.88
				$2s^22p^4(^3P)3p$ - $2s^22p^4(^3P)6s$	$^2P^0$ - ^4P	
	Nc III			$2s^22p^3(^2D)3p$ - $2s^22p^3(^2D)4s$	'P - 'D	
				$2s^22p^3(^2D)3p$ - $2s^22p^3(^2P)3d$	^3P - ^1D	
14	Nc II	182.06-182.96	182.66	$2s^22p^4(^1D)3p$ - $2s^22p^4(^1D)5s$	$^2F^0$ - ^2D	1.67
				$2s^22p^4(^3P)3p$ - $2s^22p^4(^3P)5s$	$^4D^0$ - ^2P	
	Nc III			$2s^22p^3(^4S)3d$ - $2s^22p^3(^4S)4f$	^5D- ^5F	
15	Nc II	184.56-186.16	185.36	$2s^22p^4(^3P)3p$ - $2s^22p^4(^1D)4s$	$^2P^0$ - ^2D	2.43
				$2s^22p^4(^3P)3p$ - $2s^22p^4(^3P)4d$	$^4D^0$ - ^4P, ^2P, ^2F	
				$2s^22p^4(^1D)3p$ - $2s^22p^4(^1D)4d$	$^2F^0$ -*F	
				$2s^22p^4(^3P)3p$ - $2s^22p^4(^3P)5s$	$^4D^0$ - ^4P, ^2P	
	Nc III			$2s^22p^3(^2D)3d$ - $2s^22p^3(^2D)4f$	^3D - $^{3,1}P$, $^{3,1}D$, - $^{3,1}F$, $^{3,1}G$	
					^1G - $^{1,3}G$, $^{1,3}H$	
16	Nc II	1S7.56 -188.46	188.06	$2s^22p^4(^3P)3p$ - $2s^22p^4(^3P)4d$	$^4D^0$ - 'F, ^2F	3.09
				$2s^22p^4(^3P)3s$ - $2s^22p^4(^1D)3p$	^2P - $^2D^0$	
	Nc III			$2s^22p^3(^2P)3s$- $2s^22p^3(^2P)3p$	^1P - ^1S	
17	Ne 11	188.56-189.36	188.96	$2s^22p^4(^3P)3p$ - $2s^22p^4(^3P)5s$	$^2D^0$ - ^2P	1.56
				$2s^22p^4(^1D)3p$ - $2s^22p^4(^1D)5s$	$^2P^0$ - 2_D	
18	Ne II	190.36-191.06	190.76	$2s^22p^4(^3P)3s$ - $2s^22p^4(^1D)3p$	^2P - $^2P^0$	9.16
				$2s^22p^4(^3P)3p$ - $2s^22p^4(^3P)5s$	$^2D^0$ - ^2P, ^4P	
				$2s^22p^4(^3P)3p$ - $2s^22p^4(^3P)4d$	$^4D^0$ - 'D	
19	Ne II	91.16-191.96	191.61	$2s^22p^4(^3P)3s$ - $2s^22p^4(^1D)3p$	^2P - $^2P^0$	46.4
				$2s^22p^4(^3P)3p$ - $2s^22p^4(^3P)4d$	$^2D^0$ - ^2P	
20	Nc 11	192.56-193.36	193.01	$2s^22p^4(^3P)3s$ - $2s^22p^4(^1D)3p$	^2P - $^2P^0$	20.6
				$2s^22p^4(^1D)3p$ - $2s^22p^4(^1D)5s$	$^2D^0$ - ^2D	
				$2s^22p^4(^3P)3p$ - $2s^22p^4(^1D)3d$	$^2P^0$ - ^2S	
				$2s^22p^4(^3P)3p$ - $2s^22p^4(^3P)4d$	$^2D^0$ - ^2F	
	Ne III			$2s^22p^3(^2D)3p$ - $2s^22p^3(^2D)3d$	^1P - ^1D	
				$2s^22p^3(^2D)3d$ - $2s^22p^3(^2D)4f$	^1P - $^{1,3}P$, $^{1,3}D$	
				$2s^22p^3(^2P)3d$ - $2s^22p^3(^2P)4f$	^1F - ^1G	
					^3D - ^3D	
21	Nc II	193.46-194.16	193.86	$2s^22p^4(^3P)3s$ - $2s^22p^4(^1D)3p$	^2P - $^2P^0$	9.62
				$2s^22p^4(^3P)3p$ - $2s^22p^4(^3P)4d$	$^2D^0$ - ^4P	
				$2s^22p^4(^3P)3p$ - $2s^22p^4(^3P)5s$	$^2S^0$ - ^2P	

Feature Number	Species	Integrated λ (m)	Observed Peak λ (rim)	Configuration	Term	Emission Cross Section (x 10^{-21} cm^2)
22	Ne II	194.36-194.86	194.56	$2s^22p^4(^3P)3p - 2s^22p^4(^1D)3d$	$^2P^0 - ^2P$	1.19
	Ne III			$2s^22p^3(^4S)3d - 2s^22p^3(^4S)4f$ $2s^22p^3(^2D)4s - 2s^22p^3(^2P)4f$	$^3D - ^3F$ $^1D - ^{1,3}F$	
23	Ne III	206.16-206.96	206.56	$2s^22p^3(^2D)3s - 2s^22p^3(^2D)3p$ $2s^22p^3(^2P)3p - 2s^22p^3(^2P)3d$	$^1D - ^1D$ 3_s - ‘P	10.57
24	Ne III	208.16-208.96	208.61	$2s^22p^3(^2D^0)3p - 2s^22p^3(^2D^0)3d$	$^3D - ^3D^0$	9.34
25	Ne III	209.26-210.06	209.66	$2s^22p^3(^2D^0)3p - 2s^22p^3(^2D^0)3d$ $2s^22p^3(^2P)3p - 2s^22p^3(^2P)3d$	$^3D - ^3D^0$ ‘P - ‘s ‘D - 3_D	18.7
26	Ne III	214.66-215.56	215.16	$2s^22p3(^2D^0)3p$ - $2s^22p3(2D0)3d$ $2s^22p3(^2P)3p$ - $2s^22p3(2D)4s$	‘D - $^3F^0$ $^1P - ^1D$	1.22
27	Ne III	215.66-216.86	216.36	$2s^22p^3(^4S)3p$ - $2s^22p3(4S)3d$	5p - ^5D	1.18
28	Ne III	217.36-218.56	218.06	$2s^22p^3(^2D^0)3s - 2s^22p^3(^2D^0)3p$	‘D” - 3_P	9.4
29	Ne III	220.26-221.96	221.36	$2s^22p^3(^2D^0)3p - 2s^22p^3(^2D^0)3d$ $2s^22p^3(^2P)3p - 2s^22p^3(^2P)3d$	^3F - ‘G” $^3D - ^3F$	2.27
30	Ne 111	226.16-226.96	226.56	$2s^22p^3(^2D^0)3p - 2s^22p^3(^2D^0)3d$	$^3F - ^3F^0$	0.71
31	Ne III	227.06-227.86	227.51	$2s^22p^3(^2D)3p - 2s^22p^3(^2D)3d$	‘F - ‘G	0.94
32	Ne 111	228.16-228.76	228.46	$2s^22p^3(^2P)3p - 2s^22p^3(^2D)4s$ $2s^22p^3(^2D)3p - 2s^22p^3(^2D)3d$	‘P -‘D $^1F - ^3G$	0.39
33	Ne III	235.96-237.06	236.56	$2s^22p^3(^2P)3s - 2s^22p^3(^2P)3p$	3p - 3p	6.11
34	Ne IV	237.16-237.66	237.46			0.55
35	Ne III	246.96-247.76	247.36	$2s^22p^3(^2P)3s - 2s^22p^3(^2P)3p$ $2s^22p^3(^2P)3p - 2s^22p^3(^2D)4s$	$^1P - ^1D$ ‘D- ^1D	6.49

Feature Number	Species	Integrated λ (nm)	Observed Peak λ (nm)	Configuration	Term	Emission Cross Section (x 10^{-20} cm^2)
36	Ne III	258.66-259.96	259.36	$2s^22p^3(^4S)3s - 2s^22p^3(^4S)3p$	$^5S^0 - ^5P$	2.9
37	Ne III	260.66-261.96	261.26	$2s^22p^3(^2D^0)3s - 2s^22p^3(^2D^0)3p$	$^3D^0 - ^3F$	4.93
38	Ne III	263.46-264.86	263.96	$2s^22p^3(^2P^0)3s - 2s^22p^3(^2P^0)3p$ $2s^22p^3(^2D)3p - 2s^22p^3(^2D)3d$	$^3P^0 - ^3P$ $^3P - ^3D$	3.95
39	Ne III	267.26-268.26	267.86	$2s^22p^3(^4S^0)3s - 2s^22p^3(^4S^0)3p$	$^3S - ^3P$	10.76

TABLE 2. COMPARISON OF FUV EMISSION CROSS SECTIONS OF Ne III MEASURED AT 300 eV

Feature Number	Observed Peak λ (m)	Emission Cross Section at 300 eV (x 10“21 cm^2) This Work	Smirnov and Sharonov (1972)	Samoilov et al. (1977)
29	221.36	2.27	3.8	
30	226.56	0.71	6.2	
35	247.36	6,49	14.5	
36	259.36	2.9	3.8	5.8
37	261.26	4.93	6.2	10.3
38	263.96	3.95	6.5	7.1
39	267.86	10.76	28.5	27.0